Chemistry – A European Journal

ChemEurJ Chemistry Europe European Chemical Societies Publishing

RESEARCH ARTICLE

Cyclodextrin-Based Supramolecular Crosslinking Polymers With Multiple Ruthenium Centers for Highly Efficient Electrocatalytic Ammonia Synthesis

Wei-Heng Zhang[1] | Yong-Xue Li[1] | Xin-Yu Chen[2] | Yong Chen[1] | Ying-Ming Zhang[1] | Yu-Ping Liu[2] | Xuejian Zhang[1] | Yu Liu[1,3]

[1]College of Chemistry, State Key Laboratory of Elemento-Organic Chemistry, Nankai University, Tianjin, P. R. China | [2]College of Chemistry, Key Laboratory of Advanced Energy Materials Chemistry (Ministry of Education), Nankai University, Tianjin, P. R. China | [3]Haihe Laboratory of Sustainable Chemical Transformations, Tianjin, P. R. China

Correspondence: Yong Chen (chenyong@nankai.edu.cn) | Ying-Ming Zhang (ymzhang@nankai.edu.cn) | Yu-Ping Liu (liuypnk@nankai.edu.cn) | Xuejian Zhang (18649068623@163.com) | Yu Liu (yuliu@nankai.edu.cn)

Received: 4 November 2025 | **Revised:** 5 December 2025 | **Accepted:** 8 December 2025

Keywords: ammonia synthesis | cyclodextrin | electrocatalysis | nitrate reduction reaction

ABSTRACT

Possessing multiple catalytic sites, supramolecular polymers have received attention due to their desirable electrocatalytic activity for ammonia synthesis from NO_3^-. Herein, a covalently cross-linked supramolecular catalytic system (**Ru@POP-CD**) was synthesized by nucleophilic substitution reaction between ruthenium-coordinated phenanthroline cyclodextrin and tetrafluoroterephthalonitrile, which is not only efficiently electrocatalytic for ammonia synthesis from nitrate but also provides an effective way to combat environmental pollution. Different from noncovalently cross-linked supramolecular polymers, **Ru@POP-CD** could be kept on the electrode for cycle use and inhibit the hydrogen evolution reaction (HER), achieving a Faradaic efficiency (FE_{NH3}) of 78.5% at −0.8 V versus RHE in 0.1 M KNO_3/0.1 M KOH solution, with a NH_3 yield rate of 8.72 mg h^{-1} cm^{-2}. This superior electrocatalytic performance is attributed to the unique cyclic structure with rich hydroxyl groups of the cyclodextrin, effective affinity for anionic nitrate through hydrogen bonding and the synergistic interaction of Ru tunable d-orbitals, facilitating the electroreduction of nitrate at the electrode. Meanwhile, in neutral electrolyte (0.1 M KNO_3/0.05 M K_2SO_4), **Ru@POP-CD** still possesses highly efficient catalytic performance, with the NH_3 yield rate of 7.45 mg h^{-1} cm^{-2} and FE_{NH3} of 83.8% at −0.9 V versus RHE, showing great potential in electrochemical energy supply systems.

1 | Introduction

It is well known that synthesizing ammonia from nitrogen oxides is a current research hotspot and full of challenges [1–4]. Among the methods of ammonia synthesis [5, 6], electrocatalysis has garnered significant attention due to its high efficiency and environmental friendliness for reducing nitrogen oxides (NO_2^-, NO_3^-) from pollutants [7–11]. Compared with traditional industrial ammonia production (Haber-Bosch industrial method), electrocatalytic ammonia synthesis has the characteristics of low energy consumption and low carbon emissions [12–14], diverse and environmentally friendly raw materials [15, 16], mild reaction conditions, and high safety [17, 18], high flexibility and universal applicability [19–21]. In electrocatalysis, the constructed catalysts

Wei-Heng Zhang and Yong-Xue Li contributed equally to this work.

should be precisely regulated to control the adsorption strength of intermediates, improve the desorption efficiency of target products, suppress hydrogen evolution side reactions, and be used repeatedly [22, 23]. Therefore, more efforts have been contributed to the synthesis of selective catalysts for electrocatalytic reactions [24–26] such as nitrogen reaction reduction (NRR) and oxygen reduction reaction (ORR). Recently, covalent or noncovalent supramolecular polymers were used in electrocatalysis, which not only promote high dispersion of metals in catalysts [27, 28], increasing reactive sites [29, 30], but also provide an effective way to improve the stability of catalysts and suppress the competitive hydrogen evolution reaction (HER) [31–33]. For example, Yaghi and coworkers modified the network structure of porphyrin in 2D covalent organic frameworks (COFs) to regulate the electronic properties of the active centers for the electrocatalytic reduction of CO_2 to CO. Effective charge transport along the COF framework promotes electronic connections between remote functional groups and active sites, thereby regulating the catalytic performance of the system [34]. More recently, Shan and colleagues demonstrated that anchoring catalytic species onto polycarbazole-derived electrode substrates created a hydrophobic microenvironment that stabilized intermediates while suppressing parasitic HER in aqueous nitrate-to-ammonia conversion [16].

In the construction of supramolecular electrocatalysts, cyclodextrins (CDs) have been widely applied as an important building block [35], due to their hydrophobic cavity and hydrophilic surface [36], which selectively encapsulate guests and easily modify to achieve highly efficient constructed catalysts. For example, Stoddart and coworkers reported the preparation of cyclodextrin metal-organic frameworks (CD-MOF) through the reaction of alkali metal salts with γ-cyclodextrin, and studied the application of CD-MOF as a porous separation medium in gas absorption, separation [37], and purification [38]. We reported that a nanoreactor based on the CD-MOF could achieve efficiently catalyze the nitrate reduction reaction (NO_3RR) without metals, exhibiting good Faradaic efficiency (FE) and ammonia (NH_3) yield under mild conditions, with a maximum NH_3 yield rate up to 4.66 mg h^{-1} cm^{-2} and an FE_{NH3} of 79.3%, especially in alkaline electrolytes [39]. However, cyclodextrin complex covalently cross-linked to form supramolecular polymers for an electrocatalytic system has been rarely reported, to the best of our knowledge.

Herein, we precent a covalently cross-linked supramolecular catalytic system (**Ru@POP-CD**) synthesized by nucleophilic substitution reaction between phenanthroline cyclodextrin/ruthenium complexes and tetrafluoroterephthalonitrile. This supramolecular catalytic system can effectively catalyze (NO_3RR) with ultra-high FE_{NH3} and ammonia yield under both alkaline and neutral ambient conditions. **Ru@POP-CD** exhibited highly efficient electrocatalytic performance, where the NH_3 yield rate at −0.8 V versus RHE was up to 8.72 mg h^{-1} cm^{-2} with a FE of 78.5%, which was attributed to the unique cyclic structure of the CD, the hydroxyl groups with affinity for anionic nitrate through hydrogen bonding and the synergistic interaction of Ru tunable d-orbitals, enabling the electroreduction of nitrate at the electrode. Further experiments in 0.5 M KNO_2 electrolyte (FE_{NH3} of 89.3%, NH_3 yield rate of 12.52 mg h^{-1} cm^{-2}) revealed that the mechanism of electrocatalytic NO_3RR reduction followed the $NO_3^-\rightarrow NO_2^-\rightarrow NH_3$ process (Scheme 1). The present work demonstrates that the **Ru@POP-CD** can catalyze the nitrate reduction reaction efficiently, and it has great potential for application in electrochemical energy supply systems.

2 | Results and Discussion

Ru@HOP-CD was synthesized according to our previous report [40], and its structure was characterized by ^1H NMR, HRMS, and FTIR (Figures S1–S6). The porous **Ru@POP-CD** assembly was obtained via nucleophilic aromatic substitution of hydroxyl groups on β-CD by tetrafluoroterephthalonitrile (TFTP) [41]. **Ru@HOP-CD** and TFTP were polymerized in a suspension of K_2CO_3 in tetrahydrofuran (THF) at 80°C to provide a pale-yellow precipitate in 41.7% yield (Scheme S1). The photophysical behavior was investigated. As shown in Figure S8, two characteristic absorption peaks appeared in the UV absorption spectra of **Ru@POP-CD**. The absorption peak between 220 and 400 nm was attributed to the ligand's spin transition, and the absorption peak at 476 nm was attributed to charge transfer from the ligand to the metal. Excitation of **Ru@POP-CD** with visible light at a wavelength of 450 nm produced typical red emission peaks at 525–750 nm. The FTIR spectra and corresponding XRD patterns of the **Ru@POP-CD** complex are provided in Figures S7 and 1c, confirming that the **Ru@POP-CD** complex was successfully prepared.

The **Ru@POP-CD** complex showed a porous and fluffy aggregated structure, consisting of a large number of nanoscale particles agglomerated to form a micrometer-sized secondary structure (similar to a "grape bunch" shape) (Figure 1a, b). This macroscopic morphology suggests that the catalyst possesses a certain specific surface area and porosity (S_{BET} = 30.8m^2/g) (Figure 1c), which is favorable for the diffusion and adsorption of reactant molecules. The 200 nm scale shows that the basic unit of the catalyst is well-dispersed nanoparticles (sizes of about 50–200 nm), with relatively smooth particle surfaces and interstitial spaces between some of the particles. The homogeneous dispersion of the nanoparticles indicates that the active component of the catalyst (Ru metal particles) is well dispersed (Figure 1d,e), which avoids the "encapsulation" of the active sites caused by excessive agglomeration. The better Ru dispersion would lead to the higher number of active sites per unit mass of catalyst and the higher catalytic efficiency. Meanwhile, the XRD pattern of Ru@POP-CD shows sharp diffraction peaks indicative of a crystalline porous structure. The peaks at 2θ = 8.5°, 12.1°, and 24.3° correspond to the (100), (110), and (002) planes, respectively, which are characteristic of cyclodextrin-based polymeric frameworks. The presence of these peaks confirms the formation of an ordered polymeric framework with a regular repeating structure, as opposed to a completely amorphous material. This structural order is consistent with the formation of a well-defined porous network, which is beneficial for mass transport during electrocatalysis.

Before testing the Ru@POP-CD assembly for electrocatalytic NO_3RR activity, we established a standard curve for NH_3 concentration detection using the indophenol blue method. The NH_4Cl absorption standard curve was obtained by measuring the

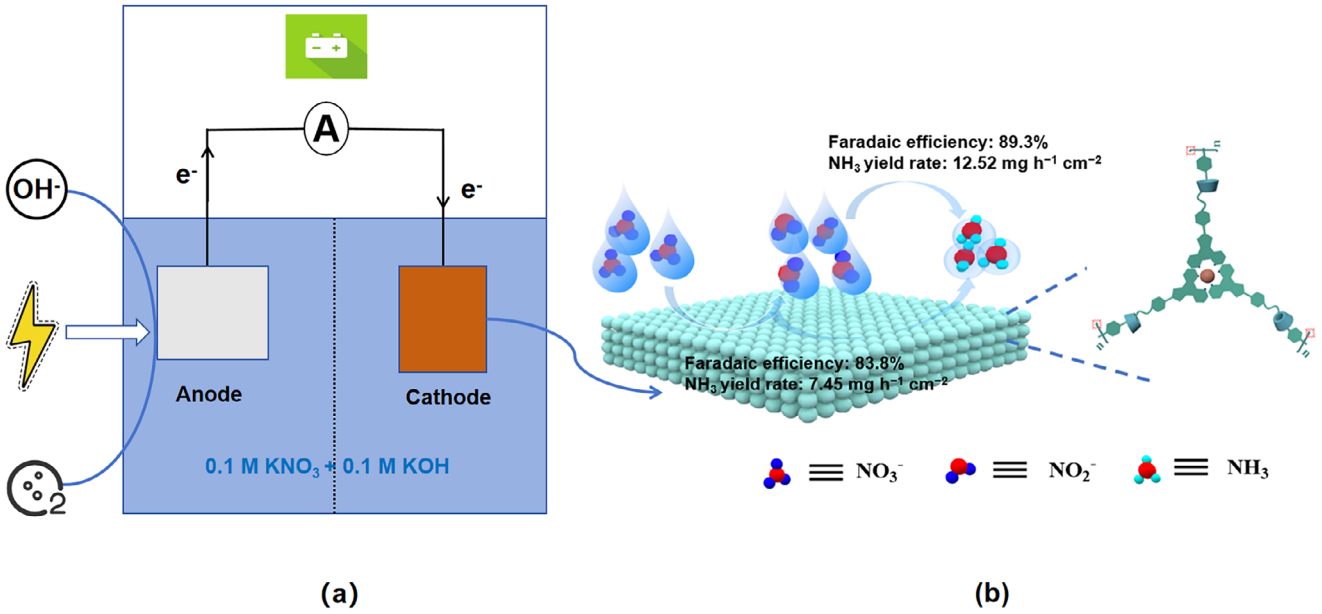

SCHEME 1 | (a) Schematic diagram of the electrocatalytic NO_3RR under ambient conditions. (b) The proposed catalytic mechanism on Ru@POP-CD.

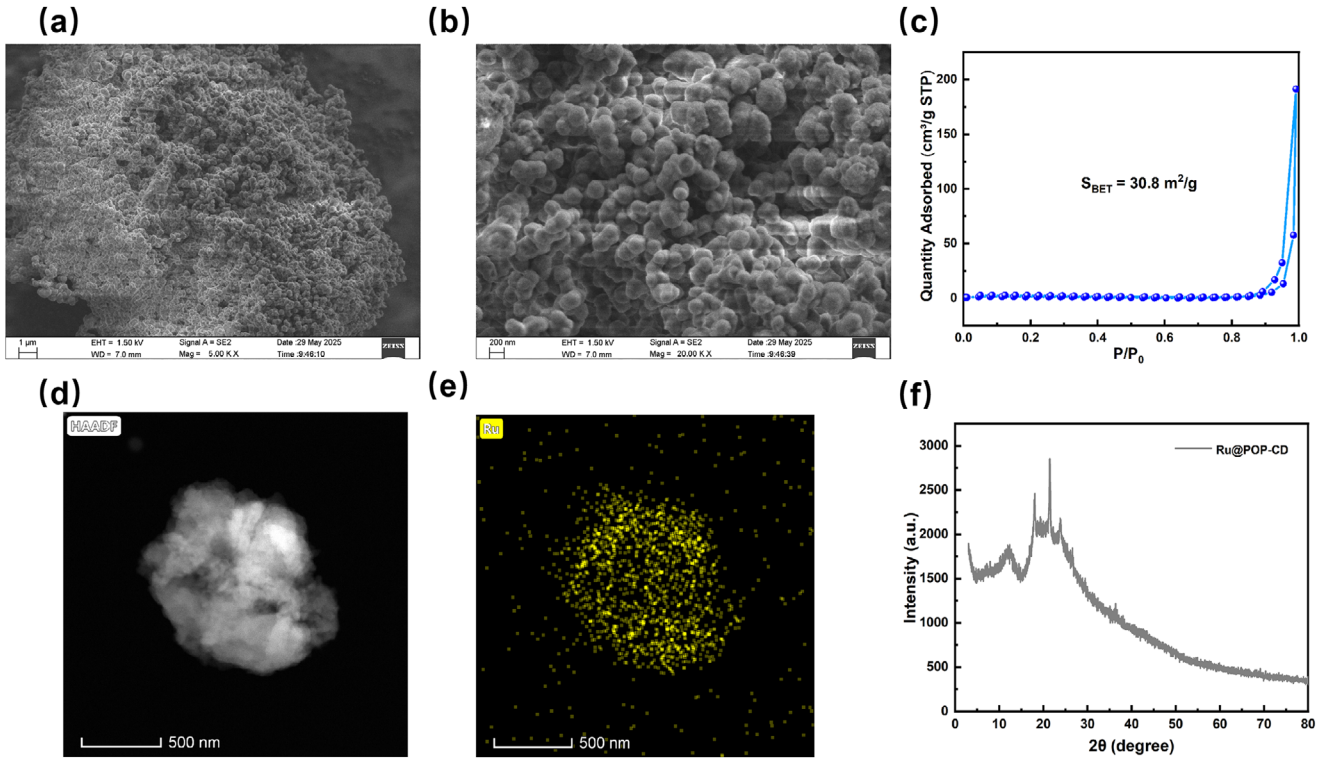

FIGURE 1 | (a) and (b) SEM images of Ru@POP-CD, (c) N_2 adsorption and desorption isotherms of Ru@POP-CD, (d) and (e) HRTEM image of Ru@POP-CD, (f) XRD pattern of Ru@POP-CD.

absorbance at wavelengths ranging from 550 to 750 nm. Next, we established a concentration-absorption standard curve of the NH_4Cl solution based on the absorbance value of the standard solution at 656 nm. Using a standard three-electrode system, we evaluated the electrocatalytic NO_3RR activity of the Ru@POP-CD assembly at room temperature and atmospheric pressure in the 0.1 M KOH electrolyte solution containing 1.0 M KNO_3 with an H-type electrolytic cell separated by a Nafion membrane. The constant potential electrolysis method was carried out at different potentials for 0.5 h. After 0.5 h of electrolysis, the cathodic electrolyte was collected, and the NH_3 produced during electrocatalysis was quantified using the indophenol blue method. We comprehensively assessed the catalytic performance of the ruthenium assembly in electrolytes of 0.1 M KNO_3/1.0 M KOH

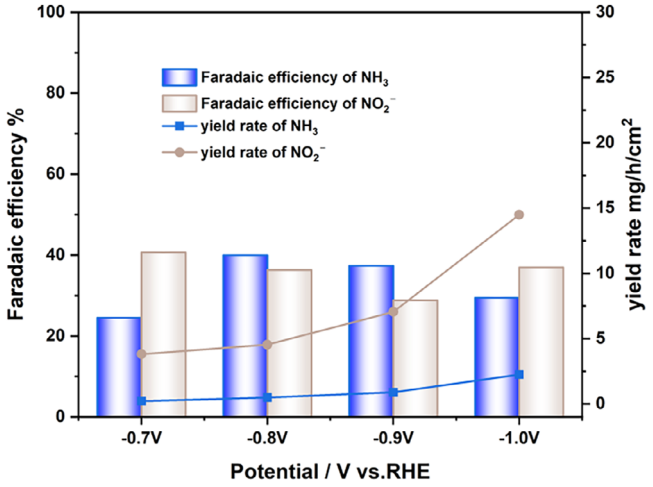

FIGURE 2 | The FEs and yields of NH_3 product and NO_2^- by-products over the Ru@POP-CD catalyst in 1.0 M KNO_3/0.1 M KOH electrolyte.

and 1.0 M KNO_3/0.1 M KOH (Figures S9, S10), respectively, under the same conditions of controlling the ionic strength. The current densities increased continuously when the negative potential was increased from −0.6 to −1.0 V versus RHE. Subsequently, the NH_3 yield rates and the FE_{NH3} were quantitatively calculated. The ruthenium assembly showed a maximum FE_{NH3} and NH_3 yield rate of 22.9% and 0.99 mg h^{-1} cm^{-2} in the 0.1 M KNO_3/1.0 M KOH electrolyte, 40.0% and 2.25 mg h^{-1} cm^{-2} in 1.0 M KNO_3/0.1 M KOH electrolyte. However, the HER was significantly reduced in 1.0 M KNO_3/0.1 M KOH electrolyte relative to in 0.1 M KNO_3/1.0 M KOH electrolyte, probably due to the selective adsorption of the ruthenium assembly for NO_3^-.

By comparing the yields and FEs of NH_3 product and NO_2^- by-products of the **Ru@POP-CD** in the 1.0 M KNO_3/0.1 M KOH electrolyte (Figure 2), it can be seen that the maximal NO_2^- yield is 6 times of the NH_3 yield, probably due to the too high concentration of NO_3^-, and the catalytic product of the **Ru@POP-CD** catalyst is mainly NO_2^-, while the yield of NH_3 is too low. To decrease the concentration of NO_3^- in the

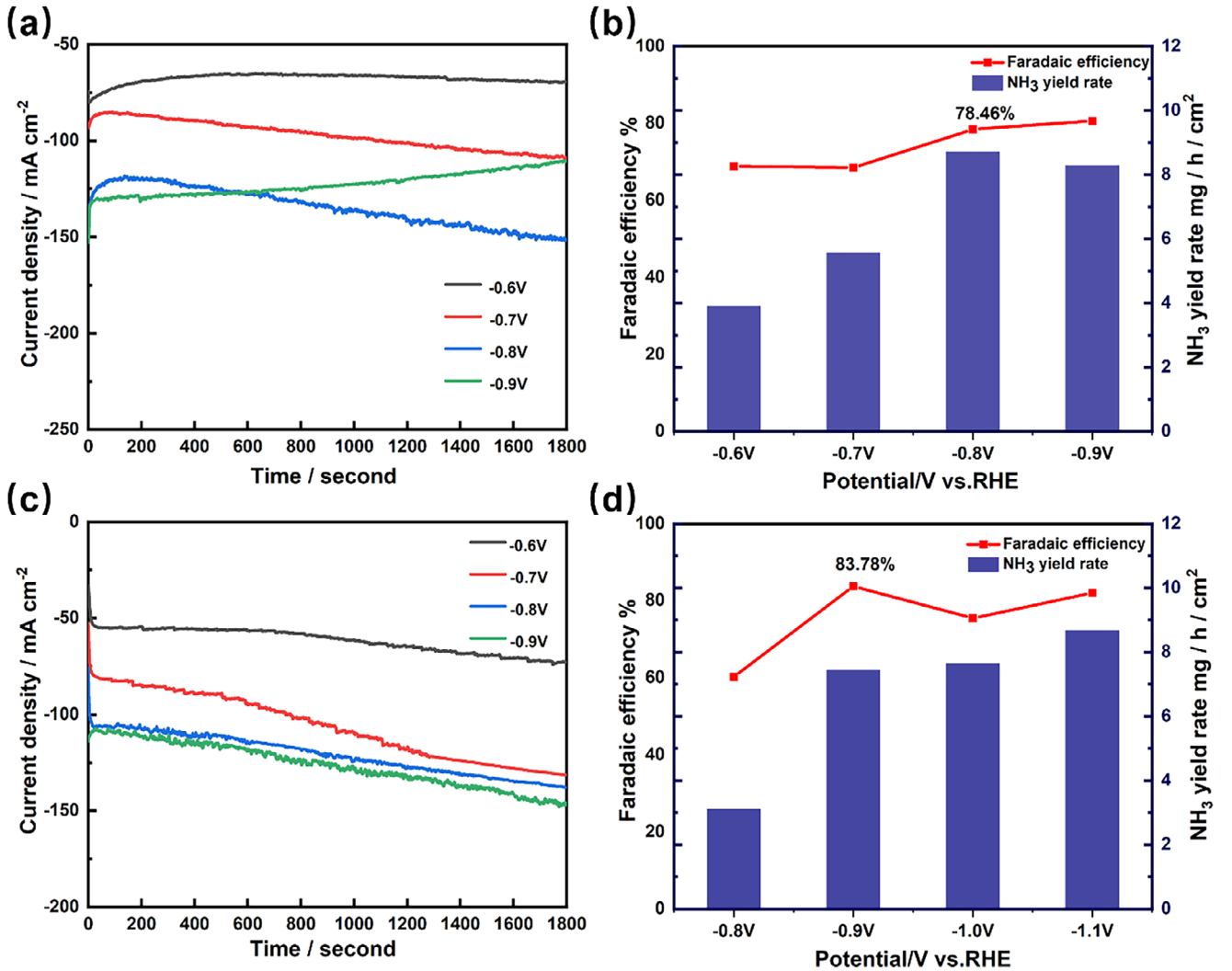

FIGURE 3 | Electrocatalytic performance evaluation of Ru@POP-CD under ambient conditions. (a) Chronoamperometric curves (b) Potential-dependent FEs (left axis) and NH_3 yield rates (right axis) of Ru@POP-CD in 0.1 M KNO_3/0.1 M KOH electrolyte (c) Chronoamperometric curves (d) Potential-dependent FEs (left axis) and NH_3 yield rates (right axis) in 0.1 M KNO_3/0.05 M K_2SO_4 electrolyte.

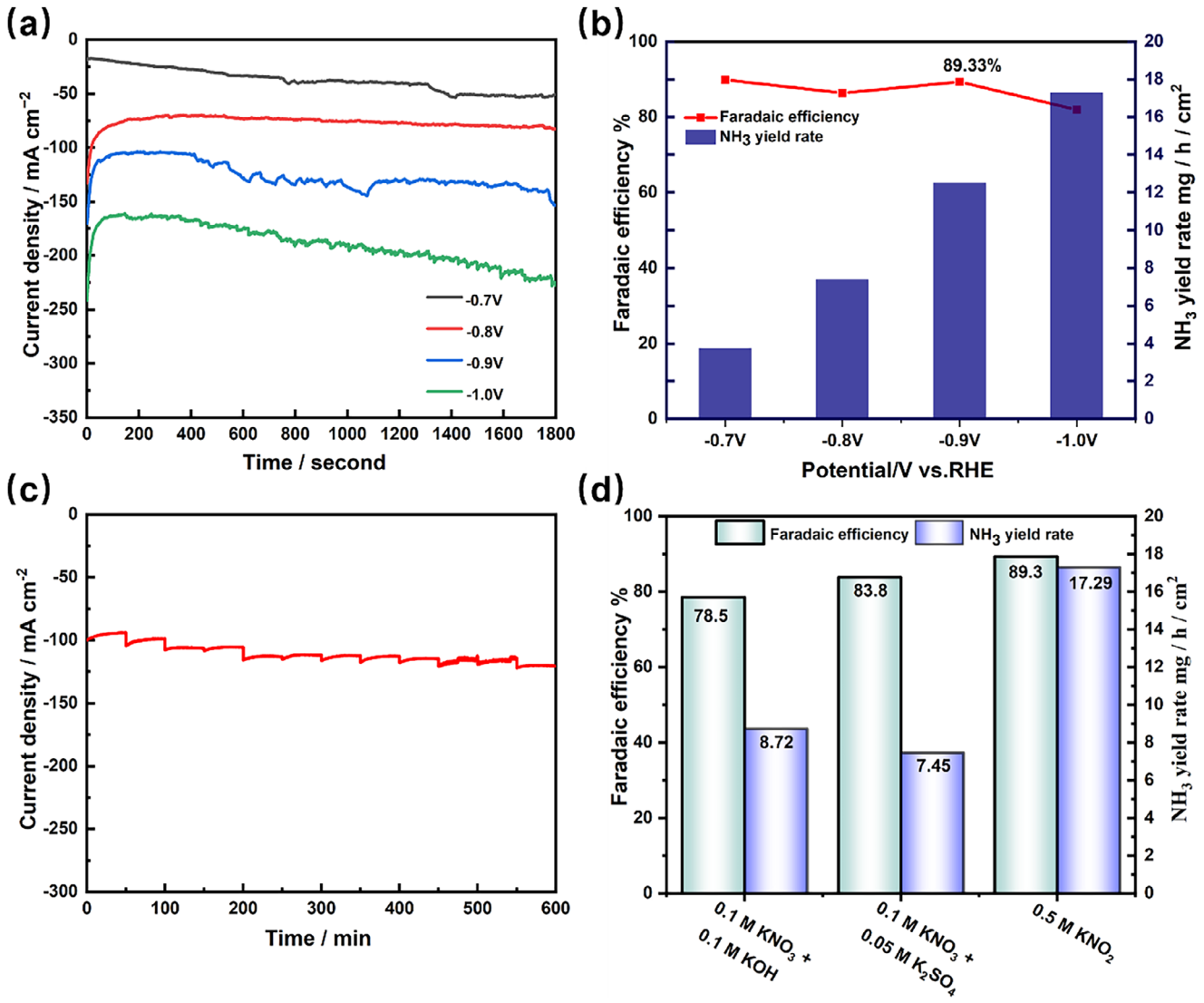

FIGURE 4 | Electrocatalytic performance comparison of Ru@POP-CD in different electrolytes under ambient conditions. (a) Chronoamperometric curves (b) Potential-dependent FEs (left axis) and NH_3 yield rates (right axis) in 0.5 M KNO_2 electrolyte. (c) Time-dependent current density curve of Ru@POP-CD during consecutive 10 h electrolysis. (d) Faraday efficiency (left axis) and ammonia yield (right axis) in three electrolytes (0.1 M KNO_3 /0.1 M KOH, 0.1 M KNO_3 /0.05 M K_2SO_4, and 0.5 M KNO_2).

electrolyte, we replaced the electrolyte with 0.1 M KNO_3/0.1 M KOH. Subsequently, the NH_3 yield rates and FEs over the catalysts were quantitatively calculated. The NH_4^+ concentration was determined through the reported indophenol blue method. Time-dependent current density curves obtained at negative potential ranging from −0.6 V to −0.9 V for 0.5 h are shown in Figure 3a. The NH_3 yield rate gradually increased when the negative potential changed from −0.6 V to −0.8 V, where the maximum NH_3 yield rate was measured to be 8.72 mg h^{-1} cm^{-2} at −0.8 V. The electrocatalytic behavior of **Ru@POP-CD** in different electrolytes was also examined (Figure 3b). The effective suppression of competing HER and favorable reaction kinetics were further confirmed by electrochemical measurements. (Figures 11(a) and (b)). Compared with in an alkaline electrolyte (0.1 M KOH/0.1 M KNO_3), the NH_3 yield rate gradually increased when the negative potential changed from −0.8 V ∼ −1.1 V (Figure 3c). The maximum values of 83.8% and 7.45 mg h^{-1} cm^{-2} of Ru@POP-CD at −0.9 V versus RHE in the neutral electrolyte (0.1 M KNO_3/0.05 M K_2SO_4) (Figure 3d). On the other hand, the experimental results also indicate that, whether in alkaline or neutral electrolyte, the **Ru@POP-CD** exhibits high catalytic efficiency and ammonia yield, demonstrating the general applicability of the phenanthroline cyclodextrin ruthenium ligand supramolecular assemblies. The catalytic activity of Ru@POP-CD was attributed to the unique cyclic structure of the CD, the hydroxyl group with affinity for anionic nitrate through hydrogen bonding and the synergistic interactions of Ru tunable d-orbitals, which facilitated the electroreduction of nitrate at the electrode.

The possible reaction pathway on Ru@POP-CD for electrocatalytic nitrate eduction to ammonia is NO_3^-→NO_2^-→NH_3, as shown by comparison experiments obtained in 0.5 M KNO_2 electrolyte. Time-dependent current density curves from −0.7 V to −1.0 V for 0.5 h are shown in Figure 4a. The NH_3 yield rate gradually increased when the negative potential changed from −0.7 V to −1.0 V, in which the maximum NH_3 yield rate was

measured to be 17.29 mg h^{-1} cm^{-2} at −1.0 V, and the FE exhibited the highest value of 89.3% at −0.9 V (Figure 4b). Continuous recycling electrolysis at −0.8 V was performed to assess the electrochemical stability of Ru@POP-CD for NO_3^- reduction at room temperature, where the current density remains basically stable in 0.1 M KOH/0.1 M KNO_3 in the course of electrolysis for 10 h (Figure 4c). The above results showed that Ru@POP-CD exhibits excellent stability electrocatalytic activity for NO_3^- reduction. The doubling of the ammonia yield in the 0.5 M KNO_2 electrolyte as compared to those in the alkaline and neutral electrolytes, on the other hand, suggests that NO_2^-→NH_3 is the decisive step in the electrocatalysis of the phenanthroline cyclodextrin ruthenium ligand supramolecular assemblies. The same is illustrated for conditions of 1.0 M KNO_3/0.1 M KOH and 0.1 M KNO_3/0.1 M KOH electrolytes (Figure 4d).

3 | Conclusion

In summary, the phenanthroline-modified cyclodextrin coordinates with Ru to form supramolecular complexes, which not only provide multiple hydroxyl groups for nucleophilic substitution reaction with tetrafluoroterephthalonitrile to form a covalently cross-linked supramolecular electrocatalytic system, but also provides hydrogen bonding sites for electrocatalysis through the synergistic interactions of hydrogen bonding and Ru. The **Ru@POP-CD** supramolecular catalyst as cathode materials to realize effective NO_3RR with favorable FE and NH_3 yield rate at ambient pressure and room temperature in an alkaline and neutral electrolyte, exhibiting highly efficient electrocatalytic performance, in which the NH_3 yield at −0.8 V versus RHE was up to 8.72 mg h^{-1} cm^{-2} with a FE of 78.5%, which was attributed to the unique cyclic structure of the CD, the hydroxyl group with affinity for anionic nitrate through hydrogen bonding and the synergistic interactions of Ru tunable d-orbitals, which facilitated the electroreduction of nitrate at the electrode. Meanwhile, in neutral electrolyte, **Ru@POP-CD** still possesses highly efficient catalytic performance, with the highest NH_3 yield rate of 7.45 mg h^{-1} cm^{-2} and FE of 83.8% at −0.8 V versus RHE. Comparison experiments in 0.5 M KNO_2 electrolyte (FE 89.3%, NH_3 yield 12.52 mg h^{-1} cm^{-2} at −0.9 V vs RHE) showed that the mechanism of electrocatalytic NO_3RR reduction is the NO_3^-→NO_2^-→NH_3 process. The present study provides a pathway for highly efficient ammonia synthesis through supramolecular electrocatalysis.

Acknowledgments

The authors thank the National Natural Science Foundation of China (NNSFC, Nos. 22131008), Fundamental Research Funds for the Central Universities (Nankai University), and the Haihe Laboratory of Sustainable Chemical Transformations for financial support.

Conflicts of Interest

The authors declare no conflict of interest.

Data Availability Statement

Research data are not shared.

References

1. S. H. Han, H. J. Li, T. L. Li, et al., "Ultralow Overpotential Nitrate Reduction to Ammonia via a Three-Step Relay Mechanism," *Nature Catalysis* 6 (2023): 402–414, https://doi.org/10.1038/s41929-023-00951-2.

2. M. Zhang, X. T. Cheng, Y. Duan, J. X. Chen, L. Wang, and Y. Q. Wang, "Hydration-Effect Boosted Active Hydrogen Facilitates Neutral Ammonia Electrosynthesis From Nitrate Reduction," *Advanced Functional Materials* 35 (2025): 2413070, https://doi.org/10.1002/adfm.202413070.

3. Y. Z. Yu, Y. Cheng, S. Cheng, and Z. Y. Wu, "Advanced Ruthenium-Based Electrocatalysts for NO x Reduction to Ammonia," *Advanced Materials* 37 (2025): 2412363, https://doi.org/10.1002/adma.202412363.

4. J. Zhong, H. Y. Duan, M. Q. Cai, et al., "Cascade Electrocatalytic Reduction of Nitrate to Ammonia Using Bimetallic Covalent Organic Frameworks with Tandem Active Sites," *Angewandte Chemie International Edition* (2025): e202507956.

5. S. Z. Andersen, V. Čolić, S. Yang, et al., "A Rigorous Electrochemical Ammonia Synthesis Protocol With Quantitative Isotope Measurements," *Nature* 570 (2019): 504–508, https://doi.org/10.1038/s41586-019-1260-x.

6. S. L. Meng, C. Zhang, C. Ye, et al., "Cobaloximes: Selective Nitrite Reduction Catalysts for Tandem Ammonia Synthesis," *Energy & Environmental Science* 16 (2023): 1590–1596, https://doi.org/10.1039/D2EE03956G.

7. S. Y. Yin, Z. X. Guan, Y. C. Zhu, D. Y. Guo, X. A. Chenh, and S. Wang, "Highly Efficient Electrocatalytic Nitrate Reduction to Ammonia: Group VIII-Based Catalysts," *ACS Nano* 18 (2024): 27833–27852, https://doi.org/10.1021/acsnano.4c09247.

8. Y. H. Wang, F. K. Hao, H. M. Xu, et al., "Interfacial Water Structure Modulation on Unconventional Phase Non-Precious Metal Alloy Nanostructures for Efficient Nitrate Electroreduction to Ammonia in Neutral Media," *Angewandte Chemie, International Edition* (2025): e202508617.

9. Y. L. Deng, X. Y. Mo, S. K. M. Lai, S. C. Haw, H. Y. Au-Yeung, and E. C. M. Tse, "Mechanical and Covalent Tailoring of Copper Catenanes for Selective Aqueous Nitrate-to-Ammonia Electrocatalysis," *Journal of the American Chemical Society* 147 (2025): 14316–14325, https://doi.org/10.1021/jacs.4c18547.

10. Y. X. Zhao, F. Wu, Y. X. Miao, et al., "Revealing Ammonia Quantification Minefield in Photo/Electrocatalysis," *Angewandte Chemie International Edition* 60 (2021): 21728–21731, https://doi.org/10.1002/anie.202108769.

11. T. Xie, X. He, L. He, et al., "$CoSe_2$ nanowire array enabled highly efficient electrocatalytic reduction of nitrate for ammonia synthesis. CoSe2 nanowire array enabled highly efficient electrocatalytic reduction of nitrate for ammonia synthesis," *Chinese Chemical Letters* 35 (2024): 110005, https://doi.org/10.1016/j.cclet.2024.110005.

12. Y. H. Wang, F. K. Hao, M. Z. Sun, et al., "Crystal Phase Engineering of Ultrathin Alloy Nanostructures for Highly Efficient Electroreduction of Nitrate to Ammonia. Crystal Phase Engineering of Ultrathin Alloy Nanostructures for Highly Efficient Electroreduction of Nitrate to Ammonia," *Advanced Materials* 36 (2024): 2313548, https://doi.org/10.1002/adma.202313548.

13. F. Y. Chen, A. Elgazzar, S. Pecaut, et al., "Electrochemical Nitrate Reduction to Ammonia With Cation Shuttling in a Solid Electrolyte Reactor," *Nature Catalysis* 7 (2024): 1032–1043, https://doi.org/10.1038/s41929-024-01200-w.

14. Y. Pan, H. M. Xu, H. R. Zhu, C. J. Huang, Z. J. Zhang, and G. R. Li, "Recent Advances in Electrocatalytic Reduction of Nitrate to Ammonia: Current Challenges, Resolving Strategies, and Future Perspectives," *Journal of Materials Chemistry A* 13 (2025): 21181–21232, https://doi.org/10.1039/D5TA02848E.

15. W. Q. Yang, H. Liu, X. X. Chang, et al., "Electrosynthesis of NH_3 From NO With Ampere-Level Current Density in a Pressurized Electrolyzer," *Nature Communications* 16 (2025): 1257, https://doi.org/10.1038/s41467-025-56548-9.

16. F. Q. Sun, Y. F. Gao, M. J. Li, et al., "Molecular Self-Assembly in Conductive Covalent Networks for Selective Nitrate Electroreduction to Ammonia," *Journal of the American Chemical Society* 145 (2023): 21491–21501, https://doi.org/10.1021/jacs.3c07320.

17. H. L. Zhao, P. F. Liu, X. T. Cheng, et al., "A Cu-Cu 2 O/Ni 2 P Heterostructure for Efficient Tandem Catalysis of Electrosynthesis of Ammonia From Nitrate Reduction Reaction in Neutral Medium," *Advanced Functional Materials* 35 (2025): 2425459, https://doi.org/10.1002/adfm.202425459.

18. Y. Yang, Y. T. Sun, Y. N. Wang, et al., "Self-Triggering a Locally Alkaline Microenvironment of Co_4 Fe_6 for Highly Efficient Neutral Ammonia Electrosynthesis," *Journal of the American Chemical Society* 147 (2025): 8893–8905, https://doi.org/10.1021/jacs.5c00688.

19. J. C. Wang, H. T. D. Bui, H. S. Hu, et al., "Industrial-current Ammonia Synthesis by Polarized Cuprous Cyanamide Coupled to Valorization of Glycerol at 4,000 mA cm −2," *Advanced Materials* 37 (2025): 2418451, https://doi.org/10.1002/adma.202418451.

20. H. L. Liu, S. H. Jia, L. M. Wu, et al., "Circumventing Scaling Relations via Gradient Orbital Coupling Promotes Ammonia Electrosynthesis on Cobalt Catalyst," *Angewandte Chemie International Edition* (2025): e202510478.

21. G. Z. Wu, W. Y. Zhang, R. Yu, et al., "p-d Orbital Hybridization in Ag-based Electrocatalysts for Enhanced Nitrate-to-Ammonia Conversion," *Angewandte Chemie, International Edition* 63 (2024): e202410251.

22. V. Kyriakou, I. Garagounis, A. Vourros, E. Vasileiou, and M. Stoukides, "An Electrochemical Haber-Bosch Process," *Joule* 4 (2020): 142–158.

23. Y. Ma, T. Yang, H. Zou, et al., "Synergizing Mo Single Atoms and Mo_2C Nanoparticles on CNTs Synchronizes Selectivity and Activity of Electrocatalytic N_2 Reduction to Ammonia," *Advanced Materials* 32 (2020): 2002177, https://doi.org/10.1002/adma.202002177.

24. F. Y. Chen, Z. Y. Wu, S. Gupta, et al., "Efficient Conversion of Low-concentration Nitrate Sources Into Ammonia on a Ru-dispersed Cu Nanowire Electrocatalyst," *Nature Nanotechnology* 17 (2022): 759–767, https://doi.org/10.1038/s41565-022-01121-4.

25. X. F. Cheng, J. H. He, H. Q. Ji, et al., "Coordination Symmetry Breaking of Single-Atom Catalysts for Robust and Efficient Nitrate Electroreduction to Ammonia," *Advanced Materials* 34 (2022): 2205767, https://doi.org/10.1002/adma.202205767.

26. B. X. Zhang, J. M. Wang, G. M. Liu, et al., "A Strongly Coupled Ru–CrOx Cluster–Cluster Heterostructure for Efficient Alkaline Hydrogen Electrocatalysis," *Nature Catalysis* 7 (2024): 441–451, https://doi.org/10.1038/s41929-024-01126-3.

27. Y. Yao, M. Xue, Z. Zhang, M. Zhang, Y. Wang, and F. Huang, "Gold Nanoparticles Stabilized by an Amphiphilic Pillar[5]Arene: Preparation, Self-Assembly Into Composite Microtubes in Water and Application in Green Catalysis," *Chemical Science* 4 (2013): 3667–3672, https://doi.org/10.1039/c3sc51547h.

28. C. Liu, J. Yao, C. Xiao, et al., "Electrochemiluminescent Chiral Discrimination With a Pillar[5]Arene Molecular Universal Joint-Coordinated Ruthenium Complex," *Organic Letters* 23 (2021): 3885–3890, https://doi.org/10.1021/acs.orglett.1c01016.

29. C. Yang, S. Maldonado, and C. R. J. Stephenson, "Electrocatalytic Lignin Oxidation," *ACS Catalysis* 11 (2021): 10104–10114, https://doi.org/10.1021/acscatal.1c01767.

30. X. Xiao, Z. Li, Y. Xiong, and Y. W. Yang, "IrMo Nanocluster-Doped Porous Carbon Electrocatalysts Derived From Cucurbit[6]Uril Boost Efficient Alkaline Hydrogen Evolution," *Journal of the American Chemical Society* 145 (2023): 16548–16556, https://doi.org/10.1021/jacs.3c03489.

31. S. B. Yu, Q. Qi, B. Yang, et al., "Enhancing Hydrogen Generation through Nanoconfinement of Sensitizers and Catalysts in a Homogeneous Supramolecular Organic Framework," *Small* 14 (2018): e1801037, https://doi.org/10.1002/smll.201801037.

32. X. Fan, D. Zhao, Z. Deng, et al., "Constructing Co@TiO_2 Nanoarray Heterostructure With Schottky Contact for Selective Electrocatalytic Nitrate Reduction to Ammonia," *Small* 19 (2023): 2208036.

33. Y. Liang, X. Fan, X. He, et al., "Selective Ammonia Production via Nitrite Electroreduction Over CoFe Layered Double Hydroxides-Decorated 3D TiO_2 Array," *Nano Research* 18 (2025): 94907344, https://doi.org/10.26599/NR.2025.94907344.

34. C. S. Diercks, S. Lin, N. Komienko, et al., "Reticular Electronic Tuning of Porphyrin Active Sites in Covalent Organic Frameworks for Electrocatalytic Carbon Dioxide Reduction," *Journal of the American Chemical Society* 140 (2018): 1116–1122, https://doi.org/10.1021/jacs.7b11940.

35. X. Y. Chen, H. Chen, L. Dordevic, et al., "Selective Photodimerization in a Cyclodextrin Metal–Organic Framework," *Journal of the American Chemical Society* 143 (2021): 9129–9139, https://doi.org/10.1021/jacs.1c03277.

36. Y. M. Zhang, Y. H. Liu, and Y. Liu, "Cyclodextrin-Based Multistimuli-Responsive Supramolecular Assemblies and Their Biological Functions," *Advanced Materials* 32 (2020): e1806158, https://doi.org/10.1002/adma.201806158.

37. K. J. Hartlieb, J. M. Holcroft, P. Z. Moghadam, et al., "CD-MOF: A Versatile Separation Medium," *Journal of the American Chemical Society* 138 (2016): 2292–2301, https://doi.org/10.1021/jacs.5b12860.

38. J. M. Holcroft, K. J. Hartlieb, P. Z. Moghadam, et al., "Carbohydrate-Mediated Purification of Petrochemicals. Carbohydrate-Mediated Purification of Petrochemicals," *Journal of the American Chemical Society* 137 (2015): 5706–5719, https://doi.org/10.1021/ja511878b.

39. X. Y. Dai, L. Tian, Z. X. Liu, W. S. Xu, Y. P. Liu, and Y. Liu, "Nanoreactor Based on Cyclodextrin for Direct Electrocatalyzed Ammonia Synthesis," *ACS Nano* 16 (2022): 18398–18407.

40. H. G. Fu, Y. Chen, Q. L. Yu, and Y. Liu, "A Tumor-targeting Ru/Polysaccharide/Protein Supramolecular Assembly with High Photodynamic Therapy Ability," *Chemical Communications* 55 (2019): 3148–3151, https://doi.org/10.1039/C8CC09964B.

41. A. Alsbaiee, B. J. Smith, L. Xiao, Y. Ling, D. E. Helbling, and W. R. Dichtel, "Rapid Removal of Organic Micropollutants From Water by a Porous β-cyclodextrin Polymer," *Nature* 529 (2015): 190–194, https://doi.org/10.1038/nature16185.

Supporting Information

Additional supporting information can be found online in the Supporting Information section.

Supporting File 1: Supporting Information is available from the Wiley Online Library or from the author.